Chapter 1

The Nuclear Shell Model

"The fundamental assumption of the shell model [is that] the motion of a single nucleon is governed by a potential representing the average interaction with all the other nucleons."
K. S. Krane

The liquid-drop SEMF (Lectures 4–5) describes bulk binding but cannot explain why certain proton or neutron numbers are especially stable. Just as atomic chemistry is organised by electronic shells, nuclear data show **magic numbers**

$$N, Z = 2, 8, 20, 28, 50, 82, 126 \tag{1.1}$$

at which nuclei are more tightly bound, more abundant, and more spherical than the SEMF alone predicts [6, 14, 1]. The nuclear shell model attributes those gaps to single-particle orbitals in a mean field, completed by a strong spin–orbit force.

1.1 Atomic shells as a guide

In atoms, major shells and subshells organise the periodic table. Closed shells (noble gases) are chemically inert: ionisation energies peak, radii are compact, and valence chemistry is nearly absent. Alkali metals, with a single electron outside a closed shell, share chemical behaviour because that valence electron dominates bonding.

The same logic applies to nuclei, with two important differences. First, both protons and neutrons fill independent sequences of levels (two interpenetrating Fermi seas). Second, the mean field is short-ranged and saturates, so the single-particle spectrum is not hydrogenic. Still, when N or Z reaches a magic number, separation energies jump, radii and abundances show discontinuities, and residual shell effects appear on top of the smooth SEMF [14, 6].

1.2 Empirical evidence for magic numbers

Several independent observables mark shell closures.

Binding-energy residuals. The difference between measured B/A and the SEMF shows positive peaks near magic N or Z (extra binding of closed shells). Pronounced humps appear near $N = 28$, $N = 50$, $N = 82$ and $Z = 28, 50, 82$, among others (Fig. 1.1).

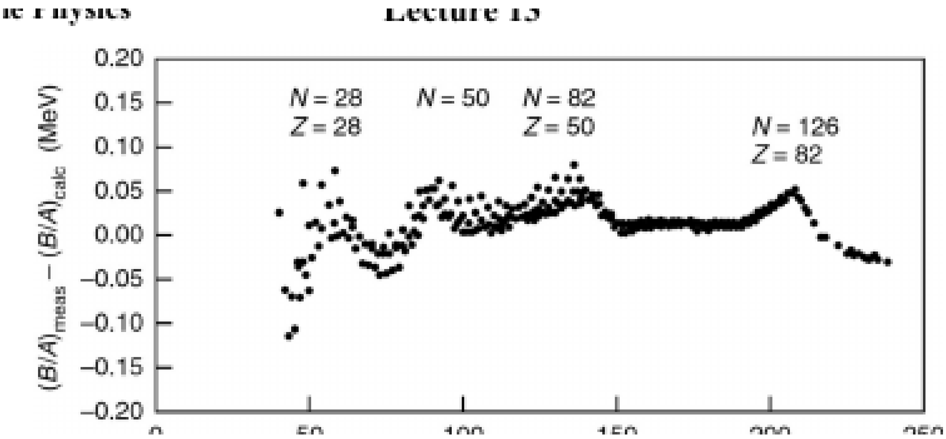

Figure 1.1: Difference between measured binding energy per nucleon and the liquid-drop (SEMF) prediction as a function of A. Peaks mark shell closures at magic N or Z (re-extracted from the full original PH5001 source page; cf. Dunlap [1] and Krane [6]).

Nuclear radii. The ratio of the measured change in nuclear radius to a smooth estimate, when N increases by two, fluctuates near $N = 20, 28, 50, 82$ (Fig. 1.2).

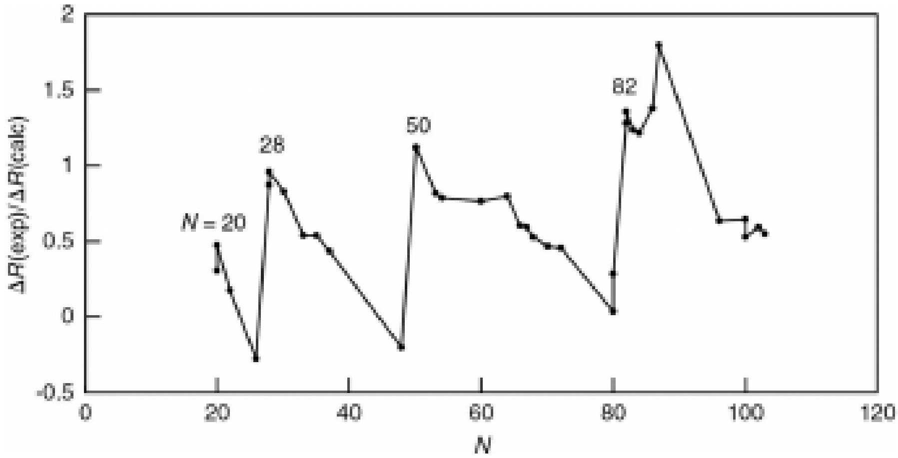

Figure 1.2: Shell effects in nuclear radii: fluctuations of $\Delta r(\text{exp})/\Delta r(\text{calc})$ near magic neutron numbers (re-extracted from the full original PH5001 source page; cf. Dunlap [1]).

Stable isotones. The number of stable isotones peaks at magic neutron numbers (Fig. 1.3): closed neutron shells favour more proton partners along the valley of stability.

Separation energies and first 2^+. S_n and S_p jump when a shell closes, analogous to atomic ionisation energies. Even–even nuclei near magic numbers also have higher-lying first 2^+ states (more rigid, spherical cores).

The experimentally identified closures are

$$2,\ 8,\ 20,\ 28,\ 50,\ 82,\ 126.$$

Beyond 126, laboratory superheavy nuclei still show evidence for further shell gaps [6, 1].

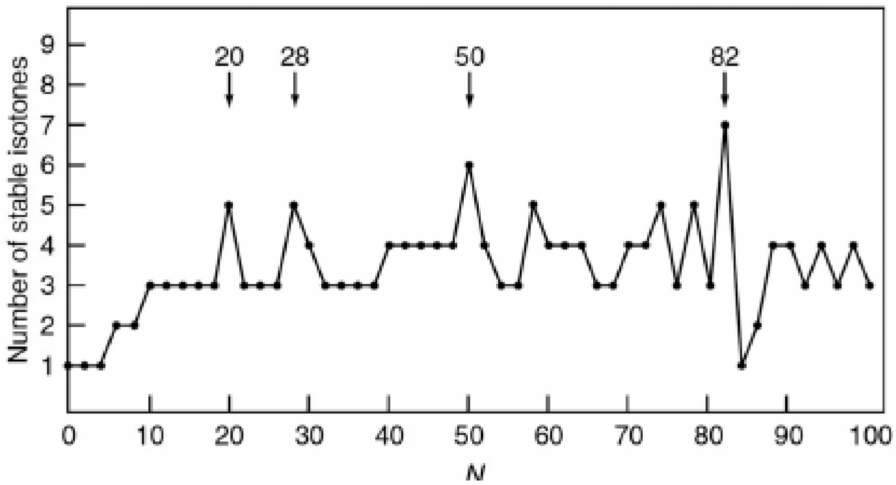

Figure 1.3: Number of stable isotones as a function of even N. Peaks at $N = 20, 28, 50, 82$ (re-extracted from the full original PH5001 source page; cf. Dunlap [1]).

Key idea

Magic numbers are experimental facts. The shell model is the mean-field theory that predicts them once a realistic single-particle potential and spin–orbit coupling are chosen.

1.3 Mean field and single-particle motion

The exact many-body Hamiltonian of A nucleons may be written schematically

$$H = \sum_{i=1}^{A} \frac{\boldsymbol{p}_i^2}{2m} + \sum_{i<j} v_{ij}, \tag{1.2}$$

where v_{ij} contains the strong interaction, Coulomb repulsion among protons, and weaker electromagnetic corrections. Solving (1.2) exactly is impossible for medium and heavy nuclei. The independent-particle approximation replaces the two-body sum by a one-body mean field $U(\boldsymbol{r})$ that represents the average interaction of one nucleon with all others:

$$H \simeq \sum_{i=1}^{A} \left[\frac{\boldsymbol{p}_i^2}{2m} + U(\boldsymbol{r}_i) \right] + V_{\text{res}}. \tag{1.3}$$

Here V_{res} collects residual interactions not absorbed into U. Pairing and collective correlations live in V_{res} and become essential away from closed shells (Lectures 13–15).

The mean field is not an externally imposed force. It is generated by the nucleons themselves, so a microscopic calculation determines the occupied orbitals and U self-consistently: the orbitals produce a density, the density produces a new field, and the cycle is repeated until both agree. The Pauli principle is essential in this picture. It forces identical nucleons to occupy different quantum states and builds separate proton and neutron Fermi seas. Nuclear saturation then explains why the depth and interior density of the mean field remain roughly independent of A, while its radius grows approximately as $A^{1/3}$.

For spherical nuclei one takes a central potential $U(\boldsymbol{r}) = V(r)$. Spherical symmetry implies that $\boldsymbol{L}^2$ and L_z commute with the single-particle Hamiltonian, so the orbital wave function separates as

$$\psi_{n\ell m}(\boldsymbol{r}) = \frac{u_{n\ell}(r)}{r}\, Y_{\ell m}(\hat{r}). \tag{1.4}$$

Substitute into the single-particle Schrödinger equation

$$-\frac{\hbar^2}{2m}\nabla^2\psi + V(r)\psi = E\psi.$$

The Laplacian in spherical coordinates yields the radial equation for $u(r)$:

$$-\frac{\hbar^2}{2m}\frac{\mathrm{d}^2u}{\mathrm{d}r^2} + \left[V(r) + \frac{\ell(\ell+1)\hbar^2}{2mr^2}\right]u = E\,u. \tag{1.5}$$

Boundary conditions are

$$u(0) = 0 \qquad \text{(regularity at the origin)} \tag{1.6}$$

and, for a bound state in a finite well,

$$u(r) \to 0 \quad \text{as} \quad r \to \infty. \tag{1.7}$$

Protons and neutrons fill independent sequences of solutions of (1.5) (two Fermi seas). Each spatial orbital of angular momentum ℓ admits $2(2\ell+1)$ identical nucleons once spin $s = \frac{1}{2}$ is included, before spin–orbit coupling is turned on. Different choices of $V(r)$ change level spacings but, without spin–orbit coupling, fail to produce the full set of magic numbers [6, 1, 13].

1.4 Infinite spherical well

Take $V = 0$ for $r < R$ and $V = \infty$ for $r \geq R$. Inside the well the potential term vanishes and (1.5) becomes

$$-\frac{\hbar^2}{2m}\frac{\mathrm{d}^2u}{\mathrm{d}r^2} + \frac{\ell(\ell+1)\hbar^2}{2mr^2}u = E\,u. \tag{1.8}$$

Define the wave number

$$k = \sqrt{\frac{2mE}{\hbar^2}}, \tag{1.9}$$

so that $E = \hbar^2k^2/(2m)$. The regular solution of (1.8) is proportional to a spherical Bessel function,

$$u(r) = A\,r\,j_\ell(kr), \tag{1.10}$$

because $j_\ell(\rho)$ satisfies the free radial equation with $\rho = kr$. The infinite wall requires $u(R) = 0$, hence

$$j_\ell(kR) = 0. \tag{1.11}$$

Let $x_{\ell,n}$ denote the nth positive zero of j_ℓ. Then

$$k_{n\ell} = \frac{x_{\ell,n}}{R}, \qquad E_{n\ell} = \frac{\hbar^2 x_{\ell,n}^2}{2mR^2}. \tag{1.12}$$

For $\ell = 0$,

$$j_0(\rho) = \frac{\sin \rho}{\rho},$$

so the zeros are $x_{0,n} = n\pi$ with $n = 1, 2, 3, \ldots$. Higher ℓ require tabulated zeros. Ordering the resulting energies produces the sequence

$$1s,\ 1p,\ 1d,\ 2s,\ 1f,\ 2p,\ 1g,\ \ldots$$

(with $1d$ and $2s$ nearly degenerate in some realisations). Unlike the Coulomb atom, there is no prohibition on $1p$, $1d$, $1f$: the nuclear mean field is not $1/r$.

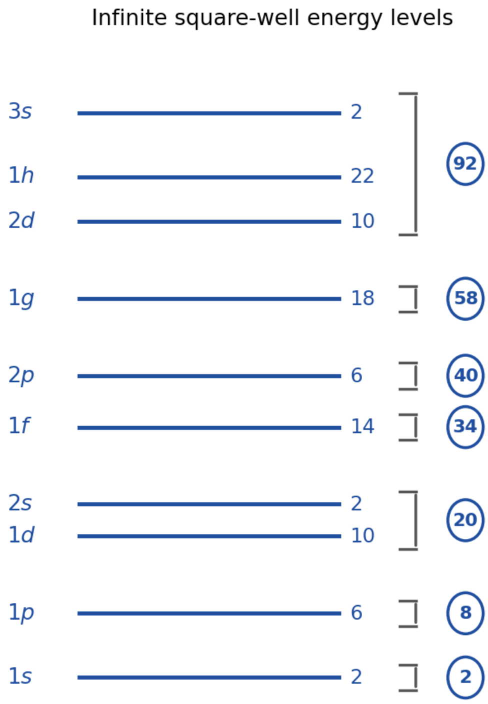

Figure 1.4: Infinite square-well single-particle levels with degeneracies and cumulative shell closures (adapted from the original PH5001 lecture figure).

Each spatial orbit of orbital angular momentum ℓ holds $2(2\ell + 1)$ identical nucleons once spin is included: $2\ell + 1$ orbital projections and two spin states. Cumulative filling therefore closes shells at

$$1s \to 2,$$
$$1s + 1p \to 2 + 6 = 8,$$
$$1s + 1p + 1d + 2s \to 8 + 10 + 2 = 20,$$

but not at 28, 50, 82, 126 [6, 1].

1.5 Isotropic harmonic oscillator

A second standard potential is the three-dimensional isotropic oscillator

$$V(r) = \tfrac{1}{2}m\omega^2 r^2. \tag{1.13}$$

In Cartesian coordinates the Hamiltonian is a sum of three independent one-dimensional oscillators,

$$H = \sum_{i=x,y,z} \left(\frac{p_i^2}{2m} + \tfrac{1}{2}m\omega^2 x_i^2 \right), \tag{1.14}$$

with eigenvalues

$$E = (n_x + n_y + n_z + \tfrac{3}{2})\hbar\omega, \qquad n_x, n_y, n_z = 0, 1, 2, \ldots. \tag{1.15}$$

Define the principal oscillator quantum number

$$N = n_x + n_y + n_z = 0, 1, 2, \ldots. \tag{1.16}$$

Then

$$E_N = \left(N + \tfrac{3}{2}\right)\hbar\omega. \tag{1.17}$$

Equivalently, in spherical coordinates one writes $N = 2n_r + \ell$ with radial quantum number $n_r = 0, 1, 2, \ldots$ and orbital angular momentum ℓ. Nuclear spectroscopic labels conventionally shift the radial count so that the lowest s orbit is called $1s$ (corresponding to $n_r = 0$).

All states with the same N are degenerate. The number of Cartesian solutions with $n_x + n_y + n_z = N$ is

$$\binom{N+2}{2} = \frac{(N+1)(N+2)}{2}. \tag{1.18}$$

Including two spin projections multiplies by 2, so the occupancy of major shell N is

$$g_N = (N+1)(N+2). \tag{1.19}$$

Explicitly:

N	Orbitals (nuclear labels)	Occupancy g_N	Cumulative
0	$1s$	2	2
1	$1p$	6	8
2	$1d, 2s$	12	20
3	$1f, 2p$	20	40
4	$1g, 2d, 3s$	30	70

Cumulative magic numbers from pure oscillator filling are therefore $2, 8, 20, 40, 70, \ldots$. Again the empirical sequence beyond 20 is missed [6, 14, 13].

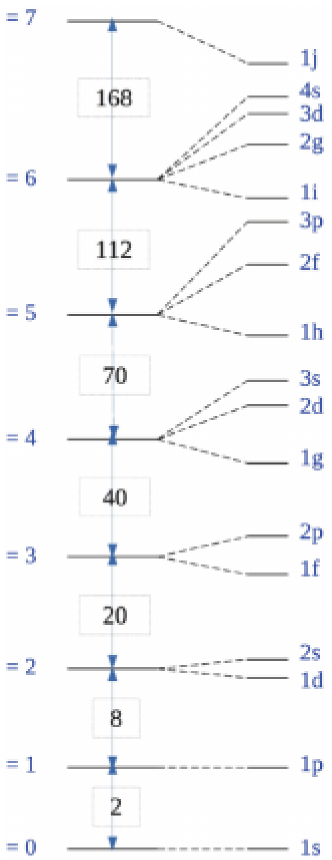

Figure 1.5: Harmonic-oscillator major shells with cumulative occupancies (adapted from the original PH5001 lecture figure).

Remark

Both the infinite well and the oscillator are unphysical as absolute walls: a particle cannot be removed by any finite energy. Real nuclei have finite separation energies $S_n, S_p \sim$ a few to tens of MeV. Finite wells (Lecture 13) fix that defect without, by themselves, fixing the magic numbers past 20.

1.6 Toward a realistic potential: Woods–Saxon shape

A finite square well allows separation but retains a discontinuous edge. Nuclear density falls smoothly over a surface thickness of order 2–3 fm. The most successful central mean field is the Woods–Saxon form

$$V(r) = -\frac{V_0}{1 + \exp[(r - R)/a]}, \tag{1.20}$$

with $R = r_0 A^{1/3}$ and diffuseness $a \sim 0.5\,\mathrm{fm}$ (Fig. 1.6). Even so, Woods–Saxon alone does not rearrange the magic numbers past 20; the essential missing piece is spin–orbit coupling [10, 6].

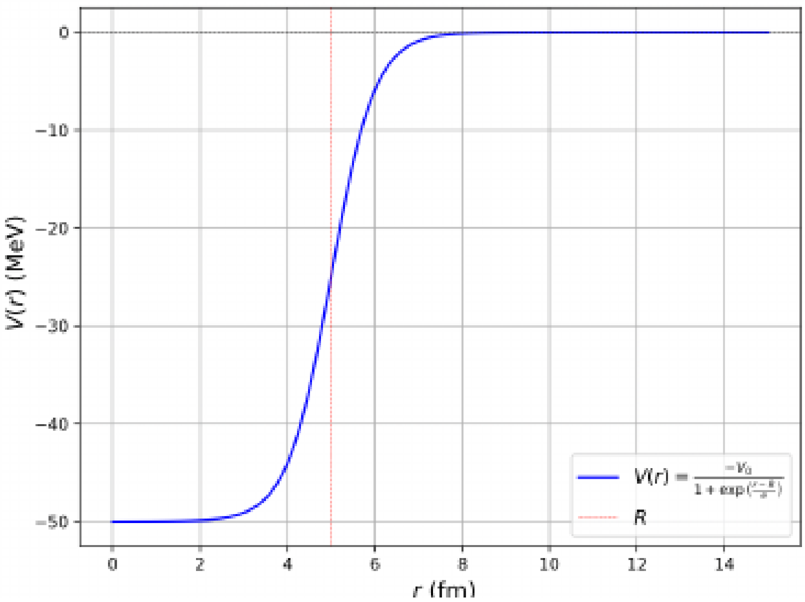

Figure 1.6: Woods–Saxon single-particle potential: flat attractive interior, diffuse surface, finite depth (adapted from the original PH5001 lecture figure; form of Woods and Saxon [10]).

1.7 Spin–orbit coupling and the correct magic numbers

Historical note: Mayer and Jensen (1949)

Maria Goeppert Mayer and, independently, **J. Hans D. Jensen** (with Haxel and Suess) showed that a strong nuclear spin–orbit force $V_{\mathrm{so}}(r)\,\boldsymbol{\ell}\cdot\boldsymbol{s}$ splits each $\ell > 0$ level into $j = \ell \pm \frac{1}{2}$ and rearranges the spectrum so that the empirical magic numbers appear. They shared the 1963 Nobel Prize in Physics with Wigner. The nuclear spin–orbit force is much stronger than its atomic electromagnetic counterpart and is a residual effect of the underlying NN interaction [6, 14].

Without spin–orbit coupling the single-particle Hamiltonian commutes with ℓ_z and s_z. Adding

$$H_{\text{so}} = f(r)\,\boldsymbol{\ell}\cdot\boldsymbol{s} \tag{1.21}$$

is often implemented phenomenologically with a radial factor proportional to the surface derivative,

$$f(r) \propto \frac{1}{r}\frac{\mathrm{d}V_{\text{WS}}}{\mathrm{d}r}. \tag{1.22}$$

Because V_{WS} changes most rapidly near $r \simeq R$, the nuclear spin–orbit interaction is surface peaked. High-ℓ orbits are especially sensitive: their centrifugal barrier pushes their probability density toward the surface, precisely where the derivative is largest. The proportionality constant and its sign are fitted so that the $j = \ell + \frac{1}{2}$ partner is the lower one. With this term, the good quantum numbers change: H no longer commutes with ℓ_z or s_z, but still commutes with ℓ^2, s^2, $\boldsymbol{j}^2$ and j_z, where

$$\boldsymbol{j} = \boldsymbol{\ell} + \boldsymbol{s}, \qquad j = \ell \pm \tfrac{1}{2} \quad (\ell \geq 1). \tag{1.23}$$

States are therefore labelled $n\ell_j$ (e.g. $1d_{5/2}$, $1d_{3/2}$).

1.7.1 Expectation value of the spin–orbit operator

Start from the operator identity obtained by expanding $\boldsymbol{j}^2 = (\boldsymbol{\ell} + \boldsymbol{s})^2$:

$$\boldsymbol{j}^2 = \boldsymbol{\ell}^2 + \boldsymbol{s}^2 + 2\,\boldsymbol{\ell}\cdot\boldsymbol{s}, \tag{1.24}$$

and therefore

$$\boldsymbol{\ell}\cdot\boldsymbol{s} = \frac{1}{2}\big(\boldsymbol{j}^2 - \boldsymbol{\ell}^2 - \boldsymbol{s}^2\big). \tag{1.25}$$

On a simultaneous eigenstate of $\boldsymbol{j}^2$, $\boldsymbol{\ell}^2$ and $\boldsymbol{s}^2$ with eigenvalues $j(j+1)\hbar^2$, $\ell(\ell+1)\hbar^2$ and $s(s+1)\hbar^2$,

$$\langle \boldsymbol{\ell}\cdot\boldsymbol{s}\rangle = \frac{\hbar^2}{2}\big[j(j+1) - \ell(\ell+1) - s(s+1)\big]. \tag{1.26}$$

For nucleons $s = \frac{1}{2}$, so $s(s+1) = \frac{3}{4}$.

Partner $j = \ell + \frac{1}{2}$.

$$j(j+1) = \Big(\ell + \tfrac{1}{2}\Big)\Big(\ell + \tfrac{3}{2}\Big) = \ell^2 + 2\ell + \tfrac{3}{4},$$

hence

$$j(j+1) - \ell(\ell+1) - s(s+1) = \big(\ell^2 + 2\ell + \tfrac{3}{4}\big) - \big(\ell^2 + \ell\big) - \tfrac{3}{4} = \ell,$$

and

$$\langle \boldsymbol{\ell}\cdot\boldsymbol{s}\rangle_{j=\ell+1/2} = \frac{\hbar^2}{2}\,\ell. \tag{1.27}$$

Partner $j = \ell - \frac{1}{2}$.

$$j(j+1) = \Big(\ell - \tfrac{1}{2}\Big)\Big(\ell + \tfrac{1}{2}\Big) = \ell^2 - \tfrac{1}{4},$$

hence

$$j(j+1) - \ell(\ell+1) - s(s+1) = (\ell^2 - \tfrac{1}{4}) - (\ell^2 + \ell) - \tfrac{3}{4} = -(\ell+1),$$

and

$$\langle \boldsymbol{\ell} \cdot \boldsymbol{s} \rangle_{j=\ell-1/2} = -\frac{\hbar^2}{2}\,(\ell+1). \tag{1.28}$$

The energy shift of each partner is $\Delta E = \langle f(r) \rangle \langle \boldsymbol{\ell} \cdot \boldsymbol{s} \rangle$. With the nuclear convention $\langle f \rangle < 0$, the $j = \ell + \frac{1}{2}$ partner is lowered and the $j = \ell - \frac{1}{2}$ partner is raised. Their splitting is

$$\Delta E_{\text{so}} = E_{j=\ell-1/2} - E_{j=\ell+1/2} = -\langle f \rangle\,\frac{\hbar^2}{2}\,(2\ell+1). \tag{1.29}$$

Large-ℓ orbits therefore split most; s states ($\ell = 0$) do not split at all.

That reordering is decisive. The high-j members of each major shell ($1f_{7/2}$, $1g_{9/2}$, $1h_{11/2}$, $1i_{13/2}$) drop into lower major shells and open gaps at the observed magic numbers [16, 17, 6, 14]:

- $1f_{7/2}$ (occupancy $2j+1=8$) alone closes a shell at $20+8=28$;
- after 28, filling $2p_{3/2}(4) + 1f_{5/2}(6) + 2p_{1/2}(2) + 1g_{9/2}(10) = 22$ yields $28+22=50$;
- the next major regrouping, including $1h_{11/2}$ (occupancy 12), yields 82;
- including $1i_{13/2}$ (occupancy 14) yields 126.

Each j subshell holds $2j+1$ identical nucleons (protons or neutrons separately). Cumulative filling:

Orbitals filled	Cumulative N or Z
$1s_{1/2}$	2
$+1p_{3/2}, 1p_{1/2}$	8
$+1d_{5/2}, 2s_{1/2}, 1d_{3/2}$	20
$+1f_{7/2}$	28
$+2p_{3/2}, 1f_{5/2}, 2p_{1/2}, 1g_{9/2}$	50
$+1g_{7/2}, 2d_{5/2}, 2d_{3/2}, 3s_{1/2}, 1h_{11/2}$	82
$+1h_{9/2}, 2f_{7/2}, \ldots, 1i_{13/2}$	126

Key idea

Central potentials alone give $2, 8, 20$. Spin–orbit coupling is required for $28, 50, 82, 126$. Remember the mechanism, not only the list: surface-peaked spin–orbit coupling lowers the high-j ($j = \ell + \frac{1}{2}$) orbit, that orbit carries $2j+1$ nucleons, and its large occupancy creates the next shell gap.

Caution

Nuclear spin–orbit ordering is opposite to the atomic fine-structure pattern for electrons: in nuclei $j = \ell + \frac{1}{2}$ lies *below* $j = \ell - \frac{1}{2}$. The strength is also orders of magnitude larger (MeV scale vs. fractions of an eV in atoms), because the force is residual strong interaction,

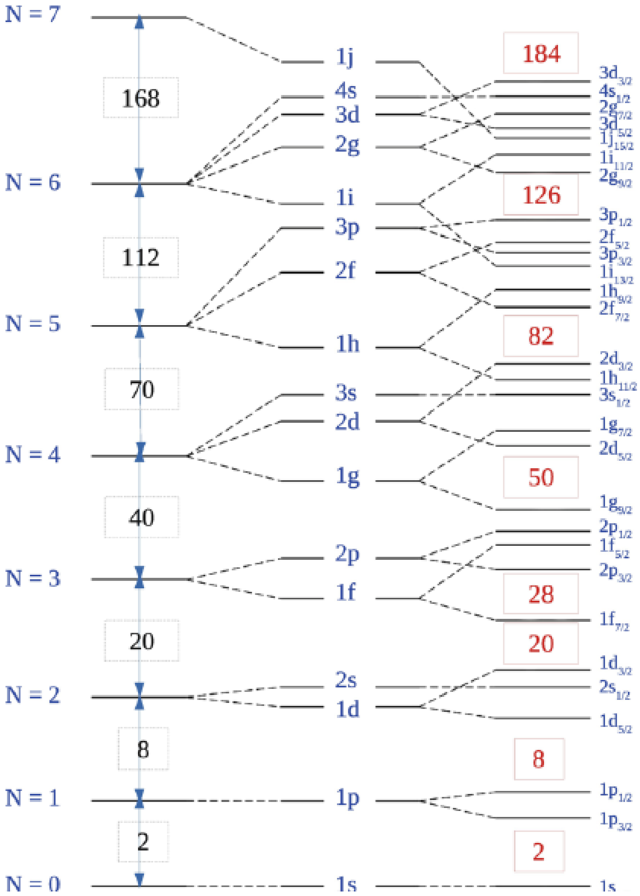

Figure 1.7: Harmonic-oscillator levels with ℓ^2 and spin–orbit splitting. Empirical magic numbers appear in red boxes (adapted from the original PH5001 lecture figure; cf. Mayer [16] and Haxel, Jensen and Suess [17]).

not electromagnetism.

1.8 Why the potential shape alone is not enough

Finite square wells, wells with rounded edges, and the Woods–Saxon form all improve separation energies and level densities relative to infinite walls. They do *not*, by themselves, produce the full magic sequence: the level order remains close to that of the oscillator or infinite well until $\boldsymbol{\ell} \cdot \boldsymbol{s}$ is added. Conversely, once a strong spin–orbit term is present, magic numbers appear for a wide class of reasonable central shapes. The empirical gaps are therefore a robust signature of spin–orbit physics, not a fine-tuned accident of one potential [6, 1].

1.9 Further physics: separation energies and double magic nuclei

Doubly magic nuclei (Z and N both magic), such as ^{4}He, ^{16}O, ^{40}Ca, ^{48}Ca, and ^{208}Pb, combine large S_n and S_p, spherical shape, and simple particle/hole spectra when one nucleon is added or removed [14, 6, 20]. They are the benchmarks against which residual interactions and ab initio methods are tested.

The one-nucleon separation energies

$$S_n(A, Z) = B(A, Z) - B(A - 1, Z), \tag{1.30}$$

$$S_p(A, Z) = B(A, Z) - B(A - 1, Z - 1) \tag{1.31}$$

jump when a shell closes, in direct analogy with atomic ionisation energies. Two-nucleon separation energies S_{2n} and S_{2p} are often smoother against odd–even staggering and therefore especially useful for mapping shell evolution far from stability.

Magic numbers need not be universal. Far from the valley of β stability, especially in neutron-rich light and medium-mass nuclei, experimental spectroscopy shows that traditional closures such as $N = 20$ or $N = 28$ can weaken or migrate ("islands of inversion"). The next predicted closures beyond $N = 126$ (e.g. $N = 184$, $Z = 114$ or nearby) underlie the search for superheavy islands of stability [14, 1].

1.10 Problems with solutions

Problem 12.1 — Occupancy of a j subshell

How many identical nucleons can occupy a $1g_{9/2}$ orbit? What cumulative magic number is completed when $1g_{9/2}$ is filled after the $N = 28$ core and the $2p, 1f_{5/2}$ orbits?

Solution 12.1

A j subshell holds $2j + 1$ identical nucleons, so

$$2j + 1 = 2 \cdot \tfrac{9}{2} + 1 = 10.$$

After the $N = 28$ core the next orbits fill as

$$\begin{aligned} 2p_{3/2} &: \ 4, \\ 1f_{5/2} &: \ 6, \\ 2p_{1/2} &: \ 2, \\ 1g_{9/2} &: \ 10, \end{aligned}$$

for a total of $4 + 6 + 2 + 10 = 22$. The cumulative closure is $28 + 22 = 50$ [6, 16].

Problem 12.2 — Why HO misses magic 28

The isotropic oscillator produces closures at $2, 8, 20, 40, \ldots$. Explain in one or two sentences how spin–orbit coupling creates a gap at 28.

Solution 12.2

In the $N = 3$ oscillator shell the spin–orbit term lowers $1f_{7/2}$ ($j = \ell + \frac{1}{2}$, $\ell = 3$) below the remaining $2p$ and $1f_{5/2}$ partners. The isolated $1f_{7/2}$ subshell holds $2j + 1 = 8$ nucleons, so a new gap opens at $20 + 8 = 28$ [6, 14, 17].

Problem 12.3 — $\ell \cdot s$ expectation values

Using $\boldsymbol{\ell} \cdot \boldsymbol{s} = \frac{1}{2}(\boldsymbol{j}^2 - \boldsymbol{\ell}^2 - \boldsymbol{s}^2)$, show that $\langle \boldsymbol{\ell} \cdot \boldsymbol{s} \rangle = \frac{1}{2}\ell\hbar^2$ for $j = \ell + \frac{1}{2}$ and $-\frac{1}{2}(\ell + 1)\hbar^2$ for $j = \ell - \frac{1}{2}$. Then show that the partner splitting is proportional to $2\ell + 1$.

Solution 12.3

With $s = \frac{1}{2}$, $s(s + 1) = \frac{3}{4}$. For $j = \ell + \frac{1}{2}$,

$$j(j + 1) = \left(\ell + \tfrac{1}{2}\right)\left(\ell + \tfrac{3}{2}\right) = \ell^2 + 2\ell + \tfrac{3}{4},$$

so

$$j(j + 1) - \ell(\ell + 1) - s(s + 1) = \ell$$

and $\langle \boldsymbol{\ell} \cdot \boldsymbol{s} \rangle = \frac{1}{2}\ell\hbar^2$. For $j = \ell - \frac{1}{2}$,

$$j(j + 1) - \ell(\ell + 1) - s(s + 1) = -(\ell + 1),$$

hence $-\frac{1}{2}(\ell + 1)\hbar^2$. The difference of the two expectation values is $\frac{1}{2}(2\ell + 1)\hbar^2$, so the energy splitting scales as $2\ell + 1$ once $\langle f(r) \rangle$ is factored out [6, 13].

Problem 12.4 — Oscillator degeneracy

Derive the occupancy $g_N = (N+1)(N+2)$ of major shell N in the isotropic three-dimensional oscillator, including spin.

Solution 12.4

The number of non-negative integer solutions of $n_x+n_y+n_z = N$ is $\binom{N+2}{2} = (N+1)(N+2)/2$. Each spatial state admits two spin projections, so

$$g_N = 2 \cdot \frac{(N+1)(N+2)}{2} = (N+1)(N+2).$$

For $N = 0, 1, 2, 3$ one recovers $2, 6, 12, 20$, and the cumulative closures $2, 8, 20, 40$ [6, 1].

Bibliography

[1] R. A. Dunlap, *An Introduction to the Physics of Nuclei and Particles* (2nd ed.), IOP Publishing, Bristol (2023), DOI: 10.1088/978-0-7503-6094-4, Ch. 3 (Nuclear composition and size).

[2] W. Demtröder, *Nuclear and Particle Physics*, Undergraduate Lecture Notes in Physics, Springer, Cham (2023).

[3] S. Petrera, *Problems and Solutions in Nuclear and Particle Physics*, UNITEXT for Physics, Springer, Cham (2019).

[4] F. Terranova, *A Modern Primer in Particle and Nuclear Physics*, Oxford University Press (2021).

[5] S. D'Auria, *Introduction to Nuclear and Particle Physics*, Undergraduate Lecture Notes in Physics, Springer, Cham (2018).

[6] K. S. Krane, *Introductory Nuclear Physics*, Wiley, New York (1988).

[7] R. Hofstadter, "Electron scattering and nuclear structure," Rev. Mod. Phys. **28**, 214 (1956).

[8] H. F. Ehrenberg, R. Hofstadter, U. Meyer-Berkhout, D. G. Ravenhall, and S. E. Sobottka, "High-Energy Electron Scattering and the Charge Distribution of Carbon-12 and Oxygen-16," Phys. Rev. **113**, 666 (1959).

[9] H. Yukawa, "On the interaction of elementary particles. I," Proc. Phys.-Math. Soc. Japan **17**, 48 (1935).

[10] R. D. Woods and D. S. Saxon, "Diffuse surface optical model for nucleon-nuclei scattering," Phys. Rev. **95**, 577 (1954).

[11] H. G. J. Moseley, "The high-frequency spectra of the elements," Phil. Mag. **26**, 1024 (1913); **27**, 703 (1914).

[12] C. F. von Weizsäcker, "Zur Theorie der Kernmassen," Z. Phys. **96**, 431 (1935).

[13] P. Cappellaro, *Introduction to Applied Nuclear Physics* (MIT OpenCourseWare / LibreTexts), CC BY-NC-SA 4.0.

[14] J.-L. Basdevant, J. Rich, and M. Spiro, *Fundamentals in Nuclear Physics: From Nuclear Structure to Cosmology*, Springer, New York (2005).

[15] D. Tong, *Particle Physics*, Lecture notes (University of Cambridge / CERN school notes).

[16] M. G. Mayer, "On closed shells in nuclei. II," Phys. Rev. **75**, 1969 (1949).

[17] O. Haxel, J. H. D. Jensen, and H. E. Suess, "On the "magic numbers" in nuclear structure," Phys. Rev. **75**, 1766 (1949).

[18] T. Schmidt, "Über die magnetischen Momente der Atomkerne," Z. Phys. **106**, 358 (1937).

[19] L. W. Nordheim, "On spins, moments, and shells in nuclei," Phys. Rev. **78**, 294 (1950).

[20] Evaluated Nuclear Structure Data File (ENSDF), National Nuclear Data Center, Brookhaven National Laboratory, `https://www.nndc.bnl.gov/ensdf/`.

[21] NuDat 3, National Nuclear Data Center, Brookhaven National Laboratory, `https://www.nndc.bnl.gov/nudat3/`.

[22] N. J. Stone, "Table of nuclear magnetic dipole and electric quadrupole moments," At. Data Nucl. Data Tables **90**, 75 (2005); updated compilations at NNDC.